Catalysis Today 424 (2023) 113843

Contents lists available at ScienceDirect

Catalysis Today

journal homepage: www.elsevier.com/locate/cattod

Enhanced activity of Cu/SiO_2 and Cu/ZrO_2 catalysts in dimethyl adipate hydrogenolysis

Jaroslav Aubrecht [a,*], Oleg Kikhtyanin [b], Violetta Pospelova [a], Iva Paterová [c], David Kubička [a,b], Federica Zaccheria [d], Nicola Scotti [d], Nicoletta Ravasio [d]

[a] Department of Petroleum Technology and Alternative Fuels, University of Chemistry and Technology Prague, Technická 5, 166 28 Prague, Czech Republic
[b] Technopark Kralupy, University of Chemistry and Technology Prague, Náměstí Georga Karse 7/2, 278 01 Kralupy nad Vltavou, Czech Republic
[c] Department of Organic Technology, University of Chemistry and Technology Prague, Technická 5, 166 28 Prague, Czech Republic
[d] CNR Institute of Chemical Sciences and Technologies "G. Natta", Via Golgi 19, 20133 Milano, Italy

ARTICLE INFO

Keywords:
Supported catalysts
Copper
Dimethyl adipate hydrogenolysis
Chemisorption-hydrolysis
Zirconia

ABSTRACT

According to green chemistry principles, the process of ester hydrogenolysis is not sustainable. It is catalysed by Adkins $CuCr_2O_3$ catalyst that brings some environmental risks. Therefore, a design of new environmentally-friendly hydrogenolysis catalysts is highly desired. We investigated eight catalysts prepared using two methods - incipient wetness impregnation (IWI) and chemisorption-hydrolysis (CH) - with a combination of two types of supports - ZrO_2 and two types of SiO_2. The preparation method affects significantly the dispersion of the resulting copper phase in case of SiO_2, and CH is essential to obtain very small and active Cu particles. On the other hand, when ZrO_2 is used, the most critical aspect is its specific surface area, and a highly dispersed copper phase is formed on the high specific surface area sample, both for CH and IWI preparation methods.

All eight prepared catalysts were investigated in dimethyl adipate hydrogenolysis to compare their activity and selectivity. Nice correlation between support – synthesis method – activity was found. ZrO_2-based catalysts and CH resulted in more active catalysts compared to SiO_2-based ones and IWI. Interestingly, Cu/SiO_2 catalyst prepared by CH was more selective to the main reaction product hexane-1,6-diol due to the presence of acid sites. In this paper, the catalyst hydrogenolysis activity was increased twice, compared to our previous experiments using Cu/ZnO prepared by deposition-precipitation.

1. Introduction

The development of environmentally-friendly catalysts is the key to the transformation of traditional chemical processes into sustainable ones for the next generations. One of the those needing a green alternative to the traditional catalyst is ester hydrogenolysis. This process is traditionally carried out over Adkins catalysts developed early in the 20th century consisting of $CuO.CuCr_2O_4$ [1–3]. The synergic effect of Cu, the active hydrogenolysis site, and Cr_2O_3, the structural promoter, ensures good catalyst stability and activity [4–6]. But, it is not desired to produce and use products containing Cr, as the presence of Cr(VI) brings large environmental and harmful impact and therefore, a novel catalyst should be designed in accordance with the green chemistry principles [7,8].

The novel catalysts should ensure good catalyst stability and high hydrogenolysis performance. As reported previously, Cu without promoters is unstable, prone to sintering, and thus affording only low ester conversion [9]. The stability of pure Cu can, however, be enhanced by using a promoter or a support [9–11]. The advantage of supported catalysts is that they allow one to use lower Cu content than the co-precipitated ones, reaching, at the same time, higher intrinsic activity [9,12]. Among them, Cu/ZrO_2 was found to be very active in dimethyl adipate hydrogenolysis [12,13], while Cu/SiO_2 was reported to have a stronger metal-support interaction that stabilizes Cu species [14].

Zirconia is a mechanically stable support that contains both acid and base sites [15,16]. When monoclinic ZrO_2 is used, the number of Lewis acid and base sites is increased due to Zr^{4+} and O^{2-} ions present [17]. Those sites can improve not only the interaction of the catalyst precursors with the support, but also the adsorption of the reacting ester and thereby facilitate hydrogenolysis [4,18]. Also, to ensure good catalyst activity, Cu/ZrO_2 interface is important [19]. Promising results were previously reported, when Cu/ZrO_2 was used in dimethyl adipate

* Corresponding author.
E-mail address: aubrechj@vscht.cz (J. Aubrecht).

https://doi.org/10.1016/j.cattod.2022.07.011
Received 31 March 2022; Received in revised form 1 July 2022; Accepted 15 July 2022
Available online 20 July 2022

hydrogenolysis [13]. On the other hand, SiO_2 provides a large surface area that could help to enhance the dispersion of metallic nanoparticles [20]. Also, the SiO_2 support has a less pronounced acid-base character, which could be beneficial since the selectivity of dimethyl adipate hydrogenolysis to hexane-1,6-diol increases with less pronounced acid-base character [13]. As both supports have their own advantages, their combination may result in a successful synergy. The synergy played the significant role in dimethyl oxalate hydrogenation to ethylene glycol when ZrO_2 was incorporated into the Cu/SiO_2 catalyst, when, in fact, it generated Cu^+ and Cu^0 active sites [16].

Besides the properties of the supports, the choice of the preparation method also influences the final catalyst properties. Incipient wetness impregnation (IWI) is a fast and user-friendly method that has been used for the preparation of hydrogenolysis catalyst [13,21–23]. In this case, the metallic phase precursor is adsorbed on the support surface from a solution of $Cu(NO_3)_2$ with pH about 3–4, as $Cu_2(OH)_3NO_3$ [24]. However, the obtained Cu nanoparticles are often rather large [13]. A more advantageous method is chemisorption-hydrolysis (CH) that allows to obtain smaller Cu nanoparticles than IWI [24]. During CH, the support is added to a basic $Cu(NH_3)_4^{2+}$ solution (pH= 9) and then slowly hydrolysed. In case of a support with a low point of zero charge, such as silica, the electrostatic interaction between the support surface and the basic solution allows the preferential adsorption of Cu^{2+} ions. This affects not only for the size of supported CuO particle but also for the interactions between the metal and the support [25].

In this paper, we wish to show how the preparation method affects the structural properties and activity and selectivity of Cu-based catalysts in dimethyl adipate hydrogenolysis. Moreover, the role of ZrO_2 and SiO_2 supports on those parameters will be answered.

2. Experimental

2.1. Catalyst preparation

We used four different supports to prepare the catalysts. ZrO_2 support named ZrO_2-1 was obtained from Saint-Gobain NorPro; ZrO_2 (3.5 % SiO_2, MELCAT XZO1521) named ZrO_2-2 was provided by MEL Chemicals; two types of silica named SiO_2-1 and SiO_2-2 were purchased from Fluka (Silica Gel 60741) and Evonik (SIPERNAT 50), respectively.

Catalysts loaded with 8 wt. % Cu were prepared by incipient wetness impregnation (IWI) and chemisorption-hydrolysis (CH).

When IWI was used, metal precursor $Cu(NO_3)_2.3H_2O$ (6.083 g) (99.0 %, Penta, s.r.o., Prague, Czechia) was dissolved in distilled water whose volume was equal to the support pore volume determined by water titration. Then, a support (18.76 g) was mixed with the precursor solution and soaked for 1 h. After that, the material was dried (T = 90 °C; t = 16 h; heating ramp of 1 °C•min^{-1}) and calcined (T = 350 °C; t = 3 h; heating ramp of 2 °C•min^{-1}).

When CH was used, $Cu(NO_3)_2.3H_2O$ (6.083 g) was dissolved in distilled water (100 ml) and 24 % aqueous ammonia (Penta, s.r.o., Prague, Czechia) was dropwise added till pH = 9, thus obtaining a $[Cu(NH_3)_4]^{2+}$ solution. Then, support (18.76 g) was added to the tetraamminocopper complex solution and the suspension was stirred for 20 min. The suspension was therefore placed in an ice bath and cooled down under stirring. Distilled water (600 ml) was added dropwise. Then, the suspension was filtered and dried at (T = 90 °C; t = 16 h; heating ramp of 1 °C•min^{-1}) and calcined (T = 350 °C; t = 3 h; heating ramp of 2 °C•min^{-1}).

2.2. Catalyst testing

All catalysts were tested in a stainless-steel autoclave (Parr, 300 ml). A catalyst (2 g) was placed into the reactor and reduced in situ at 250 °C using H_2 (99.9 %, SIAD Czech s.r.o., Czechia). Then, dimethyl adipate (DMA; 120 g) (99 %, Sigma-Aldrich, United States) was loaded. All experiments were performed at constant T = 250 °C and p_{H2} = 100 bar for 3 h. Samples were periodically taken and diluted in methanol (1:25 V/V). The diluted samples were analysed by GC-FID using Agilent 7820 with a capillary HP-5 column (30 m length, 0.32 mm i.d., 0.25 μm thick). The results were used to evaluate the catalysts performance (DMA conversion, Eq. 1) and product selectivity (Eq. 2). Due to the presence of methanol in both liquid and gaseous products, it was excluded from the quantification.

$$DMA\ \ conversion\ \ (\%) = \frac{n_{DMA,i} - n_{DMA,t}}{n_{DMA,i}} \bullet 100 \quad (1)$$

$$S_x(\%) = \frac{n_{DMA,x}}{n_{DMA,products}} \bullet 100 \quad (2)$$

where: n_{DMA} is the number of DMA moles, t is the reaction time, i is the starting reaction time, S_x is the selectivity to product x, $n_{DMA,x}$ is the number of DMA moles converted to product x and $n_{DMA,products}$ is the number of DMA moles converted to all products.

The intrinsic hydrogenolysis activity was calculated as the turnover frequency (TOF_H) using Eq. 3.

$$TOF_H = \frac{dn_{DMA,H}}{dt} \cdot \frac{\sigma_{Cu} \cdot N_A}{m_{CAT} \cdot S_{Cu}} \quad (3)$$

where: dn/dt is the change in DMA moles relative to change in time, $n_{DMA,H}$ is the number of DMA moles converted by hydrogenolysis (mol), N_A is the Avogadro constant equal to $6.022 \cdot 10^{23}$ mol^{-1}, m_{CAT} is the catalyst mass (g) and S_{Cu} is the specific copper surface area ($m^2 \cdot g_{cat}^{-1}$), t is the reaction time (initial time 0–20 min was used in calculations) (s), σ_{Cu} is the copper atom cross-section area (0.0154 nm^2).

2.3. Catalyst characterization

The elemental composition of the calcined catalysts was determined by XRF using ARL 9400 XP spectrometer equipped with a Rh lamp or by ICP – OES (ICAP6300 Duo from Thermo Fisher Scientific) with an external calibration methodology after microwave digestion of the samples.

Diffractometer PANanalytical X'Pert3 Powder and CuK_α radiation were used to determine phase composition and crystallite size of the crystalline phases. The XRD patterns were recorded in a range of 2θ = 5–70° and Scherrer's equation was used for the calculation of crystallite sizes at reflections at 2θ = 43.3° and 38.6° for Cu^0 and CuO phases, respectively [26].

Nitrogen physisorption at −196 °C performed on static volumetric adsorption system (TriFlex analyzer, Micromeritics, Norcross, USA) was used to determine textural properties of supports and calcined samples. The samples were degassed at 200 °C for 12 h prior to N_2 adsorption analysis to clean their surface. Brunauer-Emmett-Teller (BET) [27] and the Barrett-Joyner-Halenda (BJH) methods were used for the evaluation of the specific surface area (S_{BET}) and distribution of mesopores, respectively [28].

N_2O reactive frontal chromatography (N_2O-RFC) was used to determine Cu surface area (S_{Cu}) using Autochem II 2920 (Micromeritics, USA) with a quadrupole mass spectrometer RGA 200 (Prevac) which allowed to detect m/z = 28 (N_2) and m/z = 44 (N_2O) signals. The calcined catalysts were reduced in a flow of 10 vol. % H_2/Ar (30 ml·min^{-1}) at 250 °C (heating rate of 5 °C·min^{-1}) for 60 min. Then, the desorption of hydrogen occurred for 30 min at 250 °C in a flow of He (30 ml·min^{-1}) followed by cooling in He (30 ml·min^{-1}) to 90 °C. Later, the oxygen chemisorption by 3 mol. % N_2O/He (30 ml·min^{-1}) at 90 °C was performing for 30 min. The sample was then reduced by 10 mol. % H_2/Ar (30 ml·min^{-1}) with a heating to 200 °C (5 °C·min^{-1}) followed with an isotherm for 30 min. Finally, desorption of hydrogen in He (30 ml·min^{-1}) at 200 °C for 30 min, cooling in He (30 ml·min^{-1}) to 90 °C and oxygen chemisorption in 3 mol. % N_2O/He (30 ml·min^{-1}) at 90 °C for 30 min were repeated. The S_{Cu} was evaluated using the

Table 1
Physicochemical properties of the examined supports; * data above 300 °C were not considered due to the material reconstruction. PV=pore volume.

Catalyst	S_{BET} ($m^2 \cdot g^{-1}$)	PV ($ml \cdot g^{-1}$)	n_{pyr} ($\mu mol \cdot g^{-1}$)	n_{CO2} ($\mu mol \cdot g^{-1}$)
ZrO_2-1	93	0.27	75	155*
ZrO_2-2	434	0.24	496	414*
SiO_2-1	429	0.72	14	10*
SiO_2-2	556	1.90	0	0

procedure reported in [29,30]. Copper dispersion (D_{Cu}) were estimated from N_2O-RFC data using Eq. 4.

$$D_{Cu}\ (\%) = \frac{A_{N2} \bullet M_{Cu}}{w_{Cu}} \quad (4)$$

where A_{N2} is the number of N_2 moles released by the adsorption of N_2O normalized to the standard conditions (T = 0 °C; p = 101.325 kPa) (mol), w_{Cu} is the Cu mass in the measured sample (g), and M_{Cu} is the Cu atomic weight ($g \cdot mol^{-1}$).

The number of acid and base sites of supports and calcined catalyst samples were determined using temperature programmed desorption of pyridine and CO_2 (pyr-TPD; CO_2-TPD), respectively, performed on Micromeritics Instrument (AutoChem II 2920). Both desorbed pyridine or CO_2 were detected using a thermal conductivity detector (TCD) and a quadrupole mass spectrometer (MKS Cirrus 2 Analyzer). All samples were pre-treated at 300 °C and after cooling to 150 °C or 40 °C, pyridine and CO_2 were adsorbed, respectively. Then the samples were heated up to 600 °C in He and desorbed gas was analysed. Detailed procedure is described in [13].

Pyr-TPD and CO_2-TPD of reduced Cu catalysts was carried out under identical conditions as described above. Prior to the adsorption of pyridine or CO_2 the reduction of Cu catalyst proceeded in the flow of reduction gas (10 % H_2/Ar) with increasing the temperature at a rate 4 °C·min^{-1} to 250 °C and dwelling for 60 min at this temperature. After the reduction, the desorption of hydrogen in He flow at 250 °C was carried out followed by sample cooling to the adsorption temperature as described above.

TEM pictures and element maps with surface composition were determined using EFTEM Jeol 2200 FS at an accelerating voltage of 200 kV.

Table 3
Acid-base properties of the tested catalysts; * data above 350 °C were not considered due to the calcination temperature used.

Catalyst	n_{pyr} ($\mu mol \cdot g^{-1}$)	n_{CO2} ($\mu mol \cdot g^{-1}$)	n_{pyr} ($\mu mol \cdot g^{-1}$)	n_{CO2} ($\mu mol \cdot g^{-1}$)
	support		catalyst	
Cu/ZrO_2(1)-IWI	75	155	5	446 *
Cu/ZrO_2(1)-CH	75	155	6	435 *
Cu/ZrO_2(2)-CH	496	414	6	428 *
Cu/SiO_2(1)-CH	14	10	406	108 *
Cu/SiO_2(2)-CH	0	0	463	161 *
Cu/SiO_2(1)-IWI	14	10	143	93 *

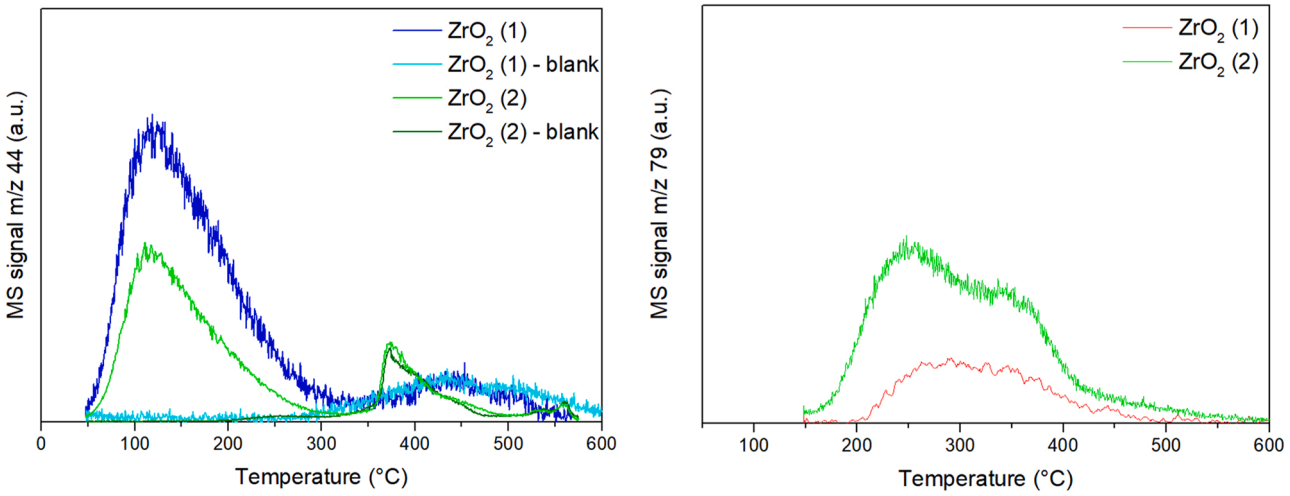

Fig. 1. CO_2-TPD (left) and pyridine-TPD (right) patterns of pure ZrO_2 supports.

Table 2
Elemental composition of the prepared catalysts; [a]XRF, [b]ICP, [c]pore volume.

Catalyst	Cu loading (%)	d_{CuO} (nm)	S_{BET} ($m^2 \cdot g^{-1}$)	PV[c] ($ml \cdot g^{-1}$)	S_{Cu} ($m^2 \cdot g_{cat}^{-1}$)	S_{Cu} ($m^2 \cdot g_{Cu}^{-1}$)	D_{Cu} (%)
Cu/ZrO_2(1)-CH	9.2[a]	12	87	0.24	3.9	42	3.5
Cu/ZrO_2(1)-IWI	9.0[a]	12	86	0.24	3.3	37	2.9
Cu/ZrO_2(2)-CH	11.4[b]	n.d.	240	0.24	2.9	25	2.7
Cu/ZrO_2(2)-IWI	7.7[b]	n.d.	307	0.30	2.7	35	2.5
Cu/SiO_2(1)-CH	8.2[b]	n.d.	310	0.56	5.6	68	5.1
Cu/SiO_2(1)-IWI	8.3[b]	n.d.	390	0.63	1.9	23	1.7
Cu/SiO_2(2)-CH	9.8[a]	n.d.	412	1.40	4.6	47	4.2
Cu/SiO_2(2)-IWI	7.9[a]	18	468	1.40	1.4	17	1.2

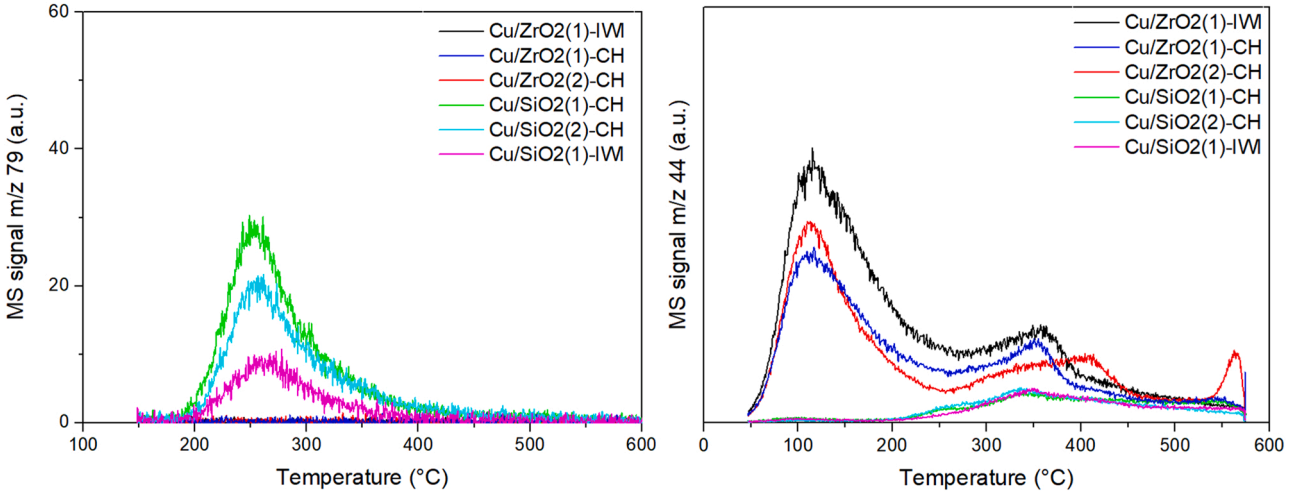

Fig. 2. pyridine-TPD (left) and CO_2-TPD (right) patterns.

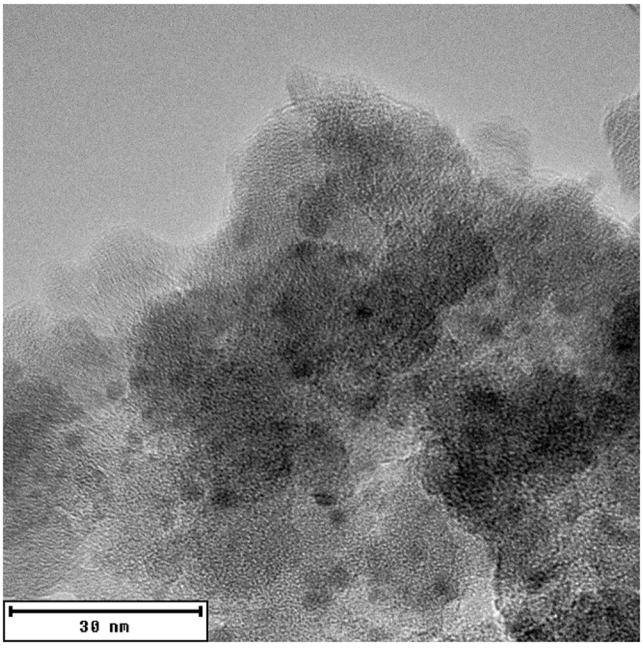

Fig. 3. Representative TEM picture of Cu/SiO_2(1)-CH confirming fine CuO dispersion.

3. Results and discussion

In the course of the development of a novel, Cr-free hydrogenolysis catalyst, two preparation methods and four supports were investigated. The CuO nanoparticles were obtained using incipient wetness impregnation (IWI) and chemisorption-hydrolysis (CH) on monoclinic-ZrO_2 (ZrO_2-1), amorphous ZrO_2 containing the 3.5 % of homogenously dispersed SiO_2 (ZrO_2-2) [31], and two SiO_2 (SiO_2-1 and SiO_2-2). This selection enabled us to evaluate: i) the effect of the preparation method on the CuO phase formation, since IWI uses mostly acidic conditions, while CH is performed under basic conditions; and ii) the effect of the support, namely crystalline m-ZrO_2 with low S_{BET} (93 $m^2.g^{-1}$) vs amorphous SiO_2 with S_{BET} about 500 $m^2.g^{-1}$. Moreover, two kinds of SiO_2 that varied in S_{BET} and pore volume (PV) (SiO_2-1 S_{BET} = 429 $m^2.g^{-1}$ and PV = 0.72 $ml.g^{-1}$ and SiO_2-2 S_{BET} = 556 $m^2.g^{-1}$ and PV = 1.90 $ml.g^{-1}$) were examined. The acid-base properties of the supports (Table 1, Fig. 1) were determined using pyr-TPD and CO_2-TPD. The pretreatment temperature prior to TPD was 300 °C, so, CO_2 released at >300 °C originated from material transformation, as blank experiments confirmed (Fig. 1-left).

The efficiency of the deposition methods and, thus, the real Cu loading were determined using XRF or ICP and the results are showed in Table 2. Nitrogen physisorption was used to determine the catalyst surface area that could affect the CuO dispersion and thus CuO nanoparticle size (Table 2). Generally, the S_{BET} increased from ca 86–470 $m^2.g^{-1}$ as the SiO_2 content increased, which means that SiO_2 might facilitate and enhance the CuO dispersion.

As highlighted in the Introduction, the two methods use different pH during the preparation with a strong influence on the catalyst properties such as CuO particle size and the strength of final metal support interaction. Therefore, the prepared samples were subjected to XRD and the size of formed CuO nanoparticles was determined (Table 2). Interestingly, no CuO (2θ = 38.6°) was detected in most the catalysts due to the formation of small CuO nanoparticles (<5 nm). Previously, XRD-invisible CuO nanoparticles of 2 nm were identified by TEM in a similar Cu/SiO_2-CH catalyst [24,32]. Larger CuO crystallites of 12 nm were detected in both Cu/ZrO_2(1)-CH and Cu/ZrO_2(1)-IWI catalysts indicating that the use of a support with a low S_{BET} negatively affects the copper dispersion even in the case of the CH method. On the other hand, the use of the high surface area zirconia (ZrO_2-2) resulted in very small Cu nanoparticles for both CH and IWI methods. In the case of Cu/SiO_2(2)-IWI, the largest nanoparticles of about 18 nm were determined. This suggests that the IWI is not a suitable preparation method to obtain small well-dispersed CuO nanoparticles on SiO_2. This can be attributed to the poor metal precursor–support electrostatic attraction during IWI caused by the low point of zero charge (PZC) in case of silica materials [13] . The attraction is driven by the difference between PZC and pH, as the PZC of SiO_2 is about 3–4.

The efficiency of deposition and interaction with the support closely relates to the final specific Cu surface area (S_{Cu}) that was investigated by N_2O chemisorption. It plays an important role, as Cu^0 is the hydrogenolysis active site (Table 2). In case of SiO_2, the S_{Cu} strongly depends on the used preparation technique as the CH catalyst had 3–4-times higher S_{Cu} than the IWI one, which was the same for copper dispersion. This is in line with the XRD results (Table 2) where much larger CuO crystallites in Cu/SiO_2(2)-IWI due to the low dispersion were observed. On the other hand, as the ZrO_2 content in the support increases, the difference between CH and IWI catalysts fades away, thus evidencing the good metal-support interaction of ZrO_2 and Cu in both environments. This is also in agreement with our previous investigation where CH was more suitable method than IWI for ZnO-supported catalysts [11].

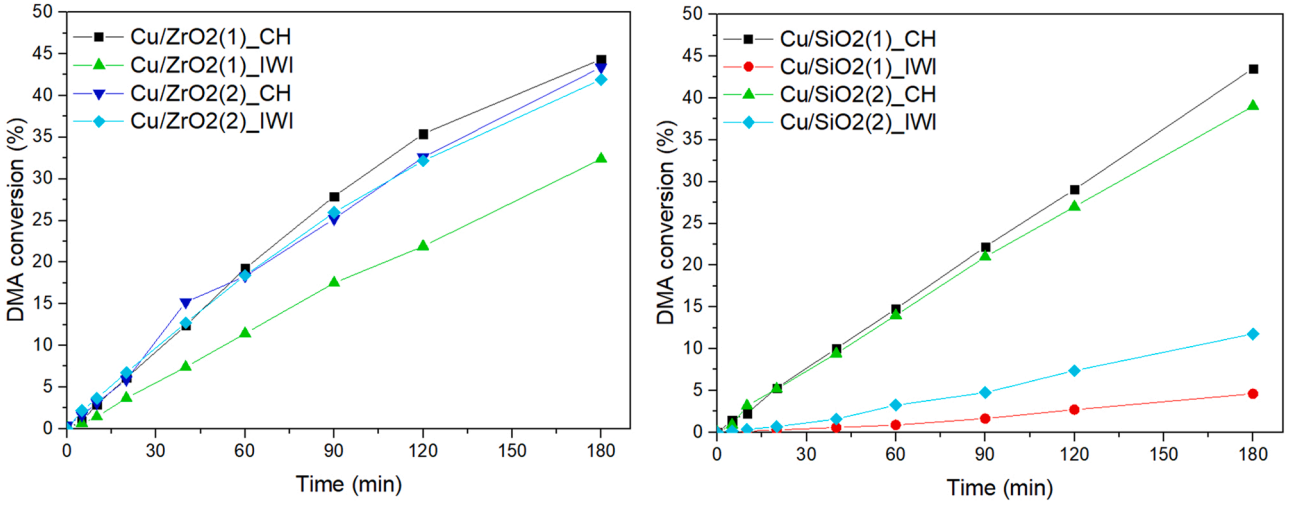

Fig. 4. DMA conversion of the tested catalysts at reaction $T = 250$ °C and $p_{H2} = 100$ bar.

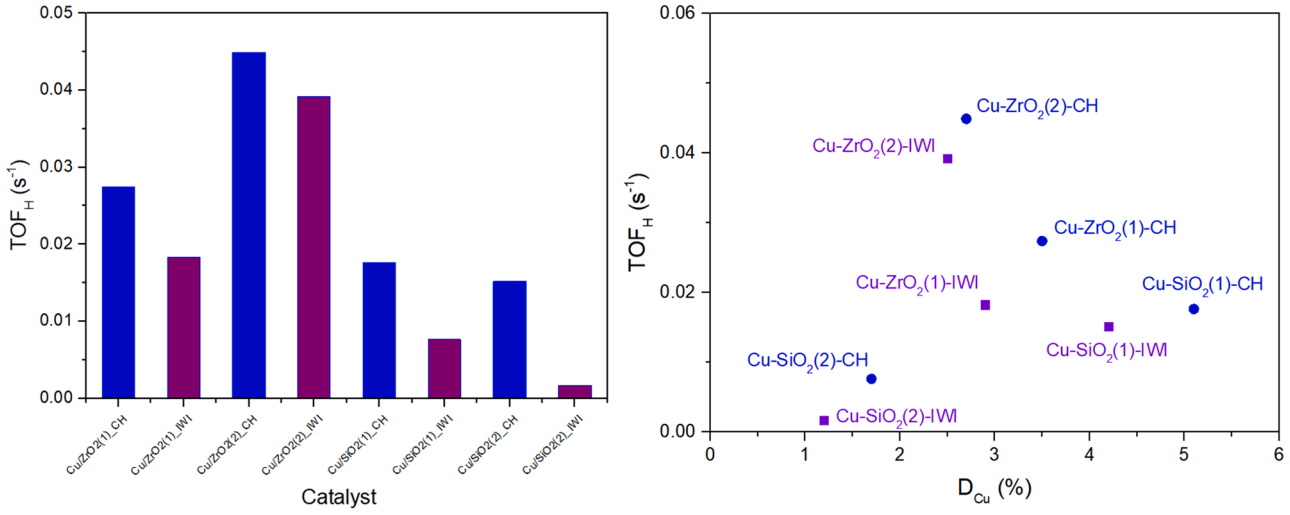

Fig. 5. Calculated catalyst activity as TOF_H within the initial 20 min of the reaction (left) and TOF_H dependence on the Cu dispersion (right) at $T = 250$ °C and $p_{H2} = 100$ bar.

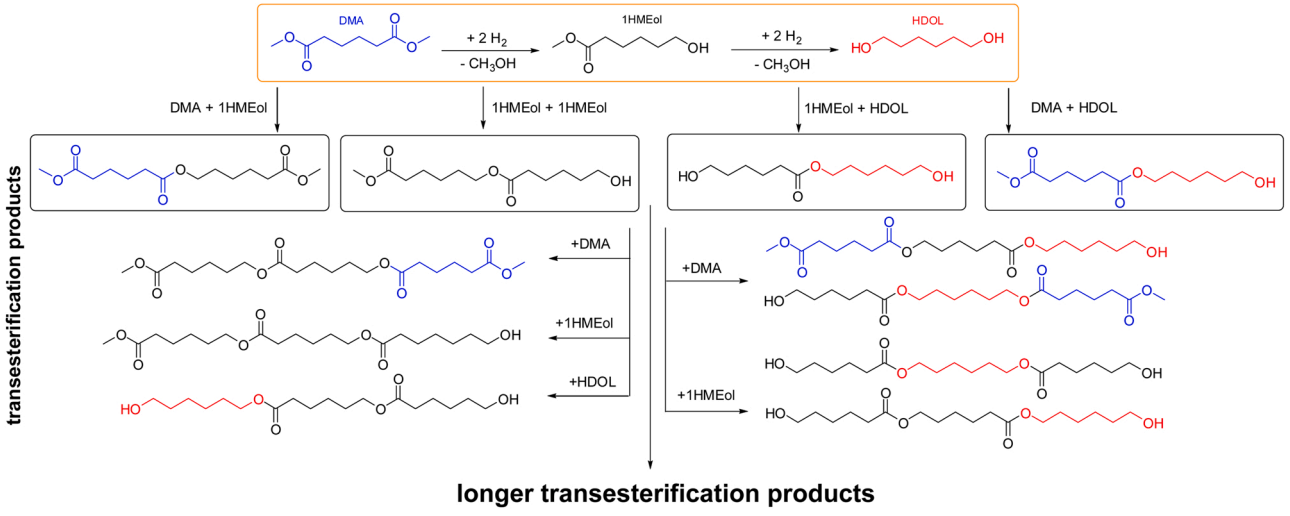

Fig. 6. Simplified reaction pathway of DMA hydrogenolysis and transesterification reactions.

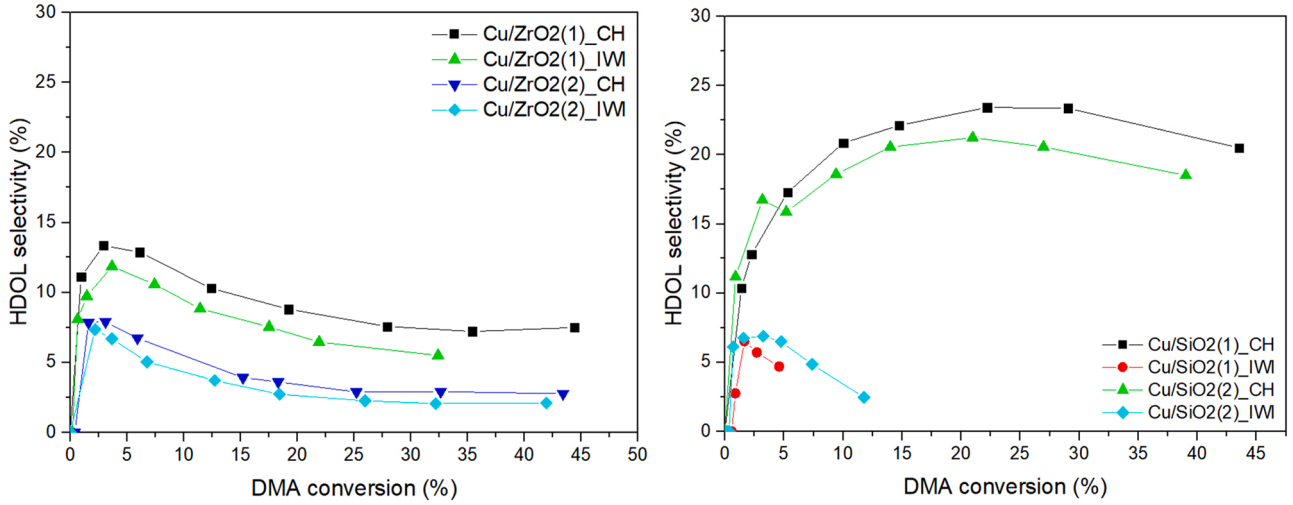

Fig. 7. HDOL selectivity reached by the tested catalysts ($T = 250$ °C and $p_{H2} = 100$ bar).

Table 4
Catalyst composition determined using STEM.

	Content, wt. %		
	Cu	ZrO_2	SiO_2
$Cu/ZrO_2(1)$-CH	9	91	–
$Cu/ZrO_2(2)$-CH	14	82	4
$Cu/SiO_2(1)$-CH	7	–	93

Recently, we have reported that acid-base sites affected the catalyst selectivity in dimethyl adipate hydrogenolysis [12,13]. To assess the influence of these parameters in supported silica- and zirconia-catalysts, the surface of the reduced catalysts was probed by pyridine and CO_2 molecules to determine the number of acid and basic sites in the case of CH and IWI Cu catalysts (Table 3 and Fig. 2).

Zirconia-based catalysts, $Cu/ZrO_2(1)$-CH, $Cu/ZrO_2(2)$-CH and $Cu/ZrO_2(2)$-IWI, had almost negligible acid character (about 6 μmol·g^{-1}), regardless of the preparation method used and the original acid character of the pure support. On the other hand, compared to pure SiO_2, the Cu incorporation increased the acid character of SiO_2-based catalysts (143–463 μmol·g^{-1}), depending on the used preparation method. The highest increase in acidity was observed in case of the CH method, with the acidity of both Cu/SiO_2-CH exceeding 400 μmol·g^{-1} (Table 3). It was previously reported that a similarly reduced Cu/SiO_2-CH catalyst had similar number of acid sites that were mostly of Lewis type [24].

While the acidity of ZrO_2-based catalysts was low, their basic character increased (398–484 μmol·g^{-1}). Interestingly, it was not affected by the used preparation method. There were two major peaks (weak basic sites at 50–250 °C and medium basic sites 250–450 °C). The first peak ascribable to weak basic sites is typical for Cu catalysts [33,34] and DFT calculation suggested that those weak sites belong to bulk Cu that adsorbs CO_2 [33]. The authors of this study [33] attributed the second peak to Cu/ZrO_2 interface formed during the calcination [33]. Moreover, Zr^{4+}/O^{2-} in monoclinic ZrO_2 is responsible for medium basic sites that are observed in that region [34].

Three of the catalysts were analyzed using TEM to investigate the homogeneity of dispersed Cu. The average composition was calculated using eight different spots on each catalyst. No Cu-rich or Cu-poor regions were detected and the average composition reached similarity with XRF or ICP. The TEM analysis showed nanoparticles in the range of 2–4 nm, that are most likely formed by CuO (Fig. 3).

3.1. Catalytic results

All prepared catalysts were reduced in situ at 250 °C and tested in an autoclave. Dimethyl adipate (DMA) hydrogenolysis was performed at 250 °C with the hydrogen pressure of 100 bar. The DMA conversions as

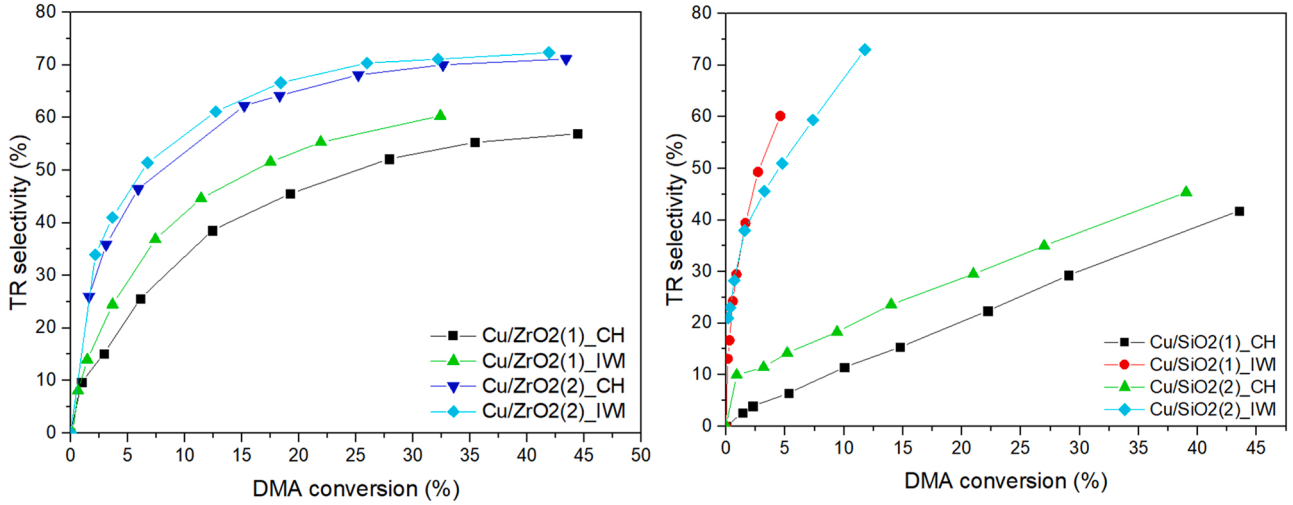

Fig. 8. Transesterification (TR) products selectivity over the tested catalysts ($T = 250$ °C and $p_{H2} = 100$ bar).

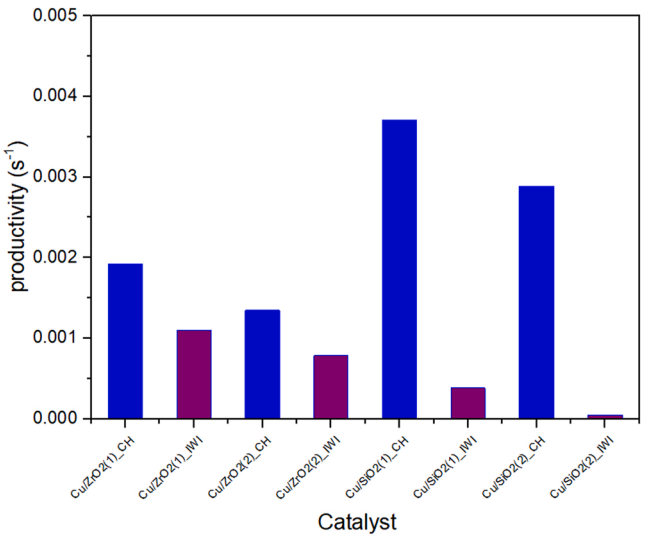

Fig. 9. Calculated productivity of catalyst active sites.

a function of reaction time are depicted in Fig. 4. The DMA conversion observed for all four CH-derived catalysts reached similar values with a maximum of 40–45 % after 180 min. On the other hand, the DMA conversion over IWI catalysts was generally lower being in the range 4–32 %. Only Cu/ZrO_2(2)-IWI was comparable with its CH counterpart, coherently with the similar copper dispersion, acid-base and textural properties of both catalysts. As discussed above, ZrO_2-based catalysts were less sensitive to the choice of the preparation method than the SiO_2-ones due to the strong metal-support interaction between Cu and zirconia, which was further confirmed by comparable DMA conversions over Cu/ZrO_2(2)-CH and Cu/ZrO_2(2)-IWI catalysts. This is in agreement with our previous results where we observed the unsuitability of the IWI method for depositing Cu on silica [13]. The Cu/SiO_2 prepared by IWI suffers from the low S_{Cu} and, consequently, poor hydrogenolysis performance. The DMA conversion over both Cu/SiO_2 prepared by CH exceeded significantly the DMA conversion over their IWI counterparts. Interestingly, the conversion grew linearly in the time span explored.

To gain a deeper insight into the activity of the differently prepared Cu phase on different supports, the hydrogenolysis turnover frequency (TOF_H) was calculated (Fig. 5-left, Eq. 3). The TOF_H gave us clear evidence that the CH catalysts (blue columns, Fig. 5-left) possessed more active Cu species than the IWI ones. The highest activity was reached by ZrO_2-based catalysts, especially by SiO_2-containing ZrO_2 (Cu/ZrO_2(2)-CH). Moreover, TOF_H was plotted as a function of copper dispersion (Fig. 5-right). Generally, TOF_H increased with the Cu dispersion, therefore, as the CH ensured better Cu dispersion, this observation underlined their effectiveness. In all cases, catalysts prepared by CH had higher Cu dispersion and, at the same time, higher TOF_H than their counterparts prepared by IWI. The catalyst hydrogenolysis activity was, however, also significantly affected by the nature of the support when even good dispersion in case of SiO_2 support did not ensure high catalyst activity.

Comparing these results with our previous studies that dealt with 10 supports and 4 synthesis methods in total, here, we enhanced the catalyst activity [11–13]. So far, the highest TOF_H of 0.024 s^{-1} was reached by Cu/ZnO-DP (deposition-precipitation) [11]. Now, Cu/ZrO_2(1)-CH and both Cu/ZrO_2(2)-CH and Cu/ZrO_2(2)-IWI outperformed it reaching 0.027–0.045 s^{-1}. Consequently, Cu/ZrO_2(2)-CH was found to be the most active catalyst in our studies being nearly twice more active than the Cu/ZnO-DP reported earlier [11].

Besides the Cu hydrogenolysis activity, the most significant difference between ZrO_2- and SiO_2-based catalysts is in their selectivity. Recently, we have described the DMA hydrogenolysis reaction pathway, where the main product hexane-1,6-diol (HDOL) is formed via methyl 6-hydroxyhexanoate (1HMEol) (Fig. 6) [12,13]. Transesterification is the main side-reaction resulting in a large group of by-products (TR) (Fig. 6). From the overall DMA-to-HDOL transformation point of view, they are rather reaction intermediates than by-products because they are hydrogenolyzed at the high DMA conversion (>80 %) to HDOL.

In this study, ZrO_2-based catalysts were less selective to HDOL (ca 5–10 %) than silica-based ones (ca 8–20 %) (Fig. 7). We identified two parameters, S_{Cu} and number of acid or basic sites, affecting the HDOL selectivity. As all ZrO_2-based catalysts had the similar acid-base character, their relative HDOL selectivity depended purely on their S_{Cu}. This specific copper surface area decreased in the order Cu/ZrO_2(1)-CH > Cu/ZrO_2(1)-IWI > Cu/ZrO_2(2)-CH > Cu/ZrO_2(2)-IWI as did also the HDOL selectivity. In other words, transesterification was preferred compared to hydrogenolysis over catalysts with lower S_{Cu}. The values of HDOL selectivity over ZrO_2-based materials nicely agree with our previously published data, where ZrO_2 was impregnated using dry impregnation [12]. These observations further support our findings that the preparation method did not influence Cu/ZrO_2 interaction. In the second case, SiO_2-based catalysts exhibited significantly increased number of acid sites (Table 4). The increased selectivity to HDOL can be due to the activation of the ester group by means of Lewis acid sites and high S_{Cu}. Both IWI-prepared SiO_2-catalysts reached low S_{Cu}, therefore, comparing the selectivity data at the same conversion, the hydrogenolysis performance was lowered in case of IWI-derived catalysts. Complementary to HDOL, TR by-products were produced with a high selectivity (Fig. 8). As the HDOL selectivity increased, the TR products selectivity decreased and vice versa.

As the silica improved the HDOL selectivity and zirconia-based catalysts were more active, the HDOL productivity was calculated (Fig. 9). Also here, the CH-derived catalysts showed better results as a higher productivity was observed than in case of IWI catalysts. Despite the lower activity, both SiO_2-CH catalysts reached a higher HDOL productivity, thus clearly showing the importance of both preparation method and the support choice.

4. Conclusions

We prepared very active Cr-free silica and zirconia supported Cu-based catalysts for dimethyl adipate hydrogenolysis, using two different preparation methods, namely IWI and CH. While IWI provided only sufficient deposition on ZrO_2, CH was a more suitable method for both types of supports. Generally, CH was a very useful method resulting in a catalyst with a high S_{Cu} and small Cu nanoparticles in comparison with IWI. Moreover, CH catalysts reached higher activity and selectivity in DMA hydrogenolysis. Although Cu supported on both types of supports afforded similar DMA conversion, the SiO_2-based catalysts provided at least a doubled selectivity to the main product, HDOL, than ZrO_2-based catalysts which was a consequence of the acid character of Cu-SiO_2 catalysts. The hydrogenolysis activity of Cu/ZrO_2(2)-CH was twice higher compared to our all previous results, in particular so far the most active Cu/ZnO prepared by deposition-precipitation. Thus, it was significantly higher than the hydrogenolysis activity of the commercial Adkins catalyst we tested previously.

CRediT authorship contribution statement

Jaroslav Aubrecht - Investigation, Methodology, Visualization, Writing – original draft; **Oleg Kikhtyanin** – Investigation; **Violetta Pospelova** - Writing – review & editing; **Iva Paterová** – Investigation; **David Kubička** – Writing – review & editing, Funding acquisition; **Federica Zaccheria** – Writing – review & editing, **Nicola Scotti**, Investigation, Writing – review & editing – and **Nicoletta Ravasio** – Writing – review & editing.

Declaration of Competing Interest

The authors declare that they have no known competing financial interests or personal relationships that could have appeared to influence the work reported in this paper.

Acknowledgements

The authors acknowledge financial support by the Czech Science Foundation (project No. GA20-28093S). The N_2O-chemisorption measurements were obtained by using Large Research Infrastructure ENREGAT supported by the Ministry of Education, Youth and Sports of the Czech Republic under project no. LM2018098.

References

[1] H. Adkins, K. Folkers, The catalytic hydrogenation of esters to alcohols, J. Am. Chem. Soc. 53 (1931) 1095–1097.
[2] H. Adkins, E.E. Burgoyne, H.J. Schneider, The copper-chromium oxide catalyst for hydrogenation, J. Am. Chem. Soc. 72 (1950) 2626–2629.
[3] H. Adkins, Catalytic hydrogenation of esters to alcohols, Org. React. 8 (1954) 1–27.
[4] P. Yuan, Z. Liu, W. Zhang, H. Sun, S. Liu, Cu-Zn/Al_2O_3 catalyst for the hydrogenation of esters to alcohols, Chin. J. Catal. 31 (2010) 769–775.
[5] T. Turek, D.L. Trimm, N.W. Cant, The catalytic hydrogenolysis of esters to alcohols, Catal. Rev. 36 (1994) 645–683.
[6] D.S. Brands, E.K. Poels, A. Bliek, Ester hydrogenolysis over promoted Cu/SiO2 catalysts, Appl. Catal. A 184 (1999) 279–289.
[7] R.D. Farris, Methyl esters in the fatty acid industry, J. Am. Oil Chem. Soc. 56 (1979) 770A–773A.
[8] P.T. Anastas, J.C. Warner, Green Chemistry: Theory and Practice, Oxford University Press, New York, 1998.
[9] J. Aubrecht, V. Pospelova, O. Kikhtyanin, L. Dubnová, D. Kubička, Do metal-oxide promoters of Cu hydrogenolysis catalysts affect the Cu intrinsic activity? Appl. Catal. A 608 (2020), 117889.
[10] V. Pospelova, J. Aubrecht, O. Kikhtyanin, K. Pacultová, D. Kubička, CuZn catalysts superior to adkins catalysts for dimethyl adipate hydrogenolysis, ChemCatChem 11 (2019) 2169–2178.
[11] V. Pospelova, J. Aubrecht, O. Kikhtyanin, D. Kubička, Towards efficient Cu/ZnO catalysts for ester hydrogenolysis: the role of synthesis method, Appl. Catal. A 624 (2021), 118320.
[12] J. Aubrecht, V. Pospelova, O. Kikhtyanin, M. Lhotka, D. Kubička, Understanding of the key properties of supported Cu-based catalysts and their influence on ester hydrogenolysis, Catal. Today 397–399 (2022) 173–181.
[13] J. Aubrecht, V. Pospelova, O. Kikhtyanin, M. Veselý, D. Kubička, Critical evaluation of parameters affecting Cu nanoparticles formation and their activity in dimethyl adipate hydrogenolysis, Catal. Today 387 (2022) 61–71.
[14] J. Gong, H. Yue, Y. Zhao, S. Zhao, L. Zhao, J. Lv, S. Wang, X. Ma, Synthesis of ethanol via syngas on Cu/SiO2 catalysts with balanced Cu0-Cu+ sites, J. Am. Chem. Soc. 134 (2012) 13922–13925.
[15] L. Castro, P. Reyes, C.M. de Correa, Synthesis and characterization of sol-Gel Cu-ZrO2 and Fe-ZrO2 catalysts, J. Sol. -Gel Sci. Technol. 25 (2002) 159–168.
[16] J. Schittkowski, K. Tölle, S. Anke, S. Stürmer, M. Muhler, On the bifunctional nature of Cu/ZrO2 catalysts applied in the hydrogenation of ethyl acetate, J. Catal. 352 (2017) 120–129.
[17] K. Pokrovski, K.T. Jung, A.T. Bell, Investigation of CO and CO_2 adsorption on tetragonal and monoclinic zirconia, Langmuir 17 (2001) 4297–4303.
[18] G. Cui, X. Meng, X. Zhang, W. Wang, S. Xu, Y. Ye, K. Tang, W. Wang, J. Zhu, M. Wei, D.G. Evans, X. Duan, Low-temperature hydrogenation of dimethyl oxalate to ethylene glycol via ternary synergistic catalysis of Cu and acid−base sites, Appl. Catal. B 248 (2019) 394–404.
[19] Y. Zhao, H. Zhang, Y. Xu, S. Wang, Y. Xu, S. Wang, X. Ma, Interface tuning of Cu+/Cu0 by zirconia for dimethyl oxalate hydrogenation to ethylene glycol over Cu/SiO2 catalyst, J. Energy Chem. 49 (2020) 248–256.
[20] B. Zhang, Y. Zhu, G. Ding, H. Zheng, Y. Li, Modification of the supported Cu/SiO2 catalyst by alkaline earth metals in the selective conversion of 1,4-butanediol to gamma-butyrolactone, Appl. Catal. A 443 (2012) 191–201.
[21] D.J. Thomas, J.T. Wehrli, M.S. Wainwright, D.L. Trimm, N.W. Cant, Hydrogenolysis of diethyl oxalate over copper-based catalysts, Appl. Catal. A 86 (1992) 101–114.
[22] L.-F. Chen, P.-J. Guo, L.-J. Zhu, M.-H. Qiao, W. Shen, H.-L. Xu, K.-N. Fan, Preparation of Cu/SBA-15 catalysts by different methods for the hydrogenolysis of dimethyl maleate to 1,4-butanediol, Appl. Catal. A 356 (2009) 129–136.
[23] J. Ding, J. Zhang, C. Zhang, K. Liu, H. Xiao, F. Kong, J. Chen, Hydrogenation of diethyl oxalate over Cu/SiO2 catalyst with enhanced activity and stability: contribution of the spatial restriction by varied pores of support, Appl. Catal. A 508 (2015) 68–79.
[24] F. Zaccheria, N. Scotti, M. Marelli, R. Psaro, N. Ravasio, Unravelling the properties of supported copper oxide: can the particle size induce acidic behaviour? Dalton Trans. 42 (2013) 1319–1328.
[25] F. Boccuzzi, A. Chiorino, G. Martra, M. Gargano, N. Ravasio, B. Carrozzini, Preparation, characterization, and activity of Cu/TiO2Catalysts. I. Influence of the preparation method on the dispersion of copper in Cu/TiO2, J. Catal. 165 (1997) 129–139.
[26] Y. Okamoto, K. Fukino, T. Imanaka, S. Teranishi, Surface characterization of copper (II) oxide-zinc oxide methanol-synthesis catalysts by X-ray photoelectron spectroscopy. 1. Precursor and calcined catalysts, J. Phys. Chem. 87 (1983) 3740–3747.
[27] S. Brunauer, P.H. Emmett, E. Teller, Adsorption of gases in multimolecular layers, J. Am. Chem. Soc. 60 (1938) 309–319.
[28] E.P. Barrett, L.G. Joyner, P.P. Halenda, The determination of pore volume and area distributions in porous substances. I. computations from nitrogen isotherms, J. Am. Chem. Soc. 73 (1951) 373–380.
[29] B. Dvorak, A. Hudec, J. Pasek, Measurement of specific copper surface-area by a pulse chromatographic technique, Collect. Czech. Chem. Commun. 54 (1989) 1514–1529.
[30] G.C. Chinchen, C.M. Hay, H.D. Vandervell, K.C. Waugh, The measurement of copper surface areas by reactive frontal chromatography, J. Catal. 103 (1987) 79–86.
[31] N. Scotti, F. Zaccheria, C. Evangelisti, R. Psaro, N. Ravasio, Dehydrogenative coupling promoted by copper catalysts: a way to optimise and upgrade bio-alcohols, Catal. Sci. Technol. 7 (2017) 1386–1393.
[32] A. Gervasini, M. Manzoli, G. Martra, A. Ponti, N. Ravasio, L. Sordelli, F. Zaccheria, Dependence of copper species on the nature of the support for dispersed CuO catalysts, J. Phys. Chem. B 110 (2006) 7851–7861.
[33] J. Yu, S. Liu, X. Mu, G. Yang, X. Luo, E. Lester, T. Wu, Cu-ZrO2 catalysts with highly dispersed Cu nanoclusters derived from ZrO2@ HKUST-1 composites for the enhanced CO_2 hydrogenation to methanol, Chem. Eng. J. 419 (2021).
[34] T. Witoon, J. Chalorngtham, P. Dumrongbunditkul, M. Chareonpanich, J. Limtrakul, CO_2 hydrogenation to methanol over Cu/ZrO2 catalysts: effects of zirconia phases, Chem. Eng. J. 293 (2016) 327–336.